Appl. Phys. A
DOI 10.1007/s00339-015-9424-5

Applied Physics A
Materials Science & Processing

INVITED PAPER

Investigating the use of Egyptian blue in Roman Egyptian portraits and panels from Tebtunis, Egypt

Monica Ganio[1] · Johanna Salvant[1] · Jane Williams[2] · Lynn Lee[3] · Oliver Cossairt[1] · Marc Walton[1]

Received: 31 March 2015 / Accepted: 7 August 2015

Abstract The use of the pigment Egyptian blue is investigated on a corpus of fifteen mummy portraits and Roman-period paintings from Tebtunis, Egypt, housed in the Phoebe A. Hearst Museum of Anthropology at the University of California, Berkeley. Egyptian blue has a strong luminescence response in the near infrared that can be exploited to created wide-field images noninvasively showing the distribution of the pigment on a work of art. A growing body of publications in the last decade highlights the increasing use of this tool and its sensitive detection limits. However, the technique is not wavelength specific. Both excitation and emission occur in a broad range. Although Egyptian blue has a strong emission in the NIR, a myriad of other compounds may emit light in this spectral region when excited in the visible. The limited number of studies including complementary analysis to verify the presence of Egyptian blue does not allow its identification on the basis of NIR luminescence alone. Through the use of in situ X-ray fluorescence and X-ray diffraction, and scanning electron microscopy/energy-dispersive spectroscopy of cross sections, this paper confirms the identification of Egyptian blue by NIR luminescence in unexpected areas, i.e., those not blue in appearance.

✉ Marc Walton
marc.walton@northwestern.edu

[1] Center for Scientific Studies in the Arts, Northwestern University, Chicago, IL, USA

[2] Phoebe A. Hearst Museum of Anthropology, University of California, Berkeley, Berkeley, CA, USA

[3] Getty Conservation Institute, Los Angeles, CA, USA

1 Introduction

At the end of nineteenth century, the University of California, Berkeley, became actively involved in archeological excavations with the intent of building collections for a new university museum, now the Phoebe A. Hearst Museum of Anthropology (PAHMA) [1]. One of these excavation campaigns, at the site of Tebtunis (modern Umm el-Breigat) in the Fayum region of Egypt, was undertaken by a pair of Oxonian papyrologists, Bernard P. Grenfell and Arthur S. Hunt [2]. Despite the fact that Grenfell and Hunt did not record the exact context of the Tebtunis artifacts in detail, this excavation yielded 15 Roman Egyptian portraits and painting fragments from this single location. Today this corpus of paintings remains one of the largest groupings of Roman Egyptian mummy portraits and paintings to survive intact since their excavation with a corresponding strong link to their original archeological context.

The portraits have all been stylistically dated to the second century AD [3, 4]. In Roman Egypt, such portraits were placed over the face of the deceased and tied into the cloth wrappings during mummification [5]. A fragmentary painted panel depicting a priest accompanied by a child (#6-21387), also studied here, possibly dates to the third century AD and had a function in antiquity that is not entirely understood. These paintings have undergone little treatment intervention or study while at the PAHMA, and none show evidence of restoration coatings typical of historic field treatments, such as overall consolidation with paraffin. With their relatively pristine conservation history and strong contextual information, these portraits are ideally suited to the study of their pigments, layering structure, and binding media to establish a more complete understanding of both Roman Egyptian painting practices and the larger social context of their use.

Published online: 14 August 2015

This study focuses on a single blue pigment, known as Egyptian blue. The pigment, consisting of cuprorivaite ($CaCuSi_4O_{10}$) [6, 7] with variable amount of wollastonite ($CaSiO_3$), Cu-rich glass and cuprite (Cu_2O), or tenorite (CuO) [8], is so far the first synthetic pigment ever produced by man. In the Old Kingdom, the source of copper was most likely malachite, azurite, or a mixture of both [8]. Starting in the 18th dynasty, the increasing amount of tin suggests a technological change, with the use of bronze fillings/scrapings or copper-containing minerals as copper source [8]. Experimental reproduction in laboratory, obtained by firing a mixture of quartz powder, copper (II) carbonate hydroxide 1-hydrate (i.e., artificial malachite), calcium carbonate, and anhydrous sodium carbonate [9], has highlighted the need for a constant control of the furnace environment with particular regard to the temperature [9–11]. The first documented appearance of the pigment dates to dynasty 0 in Egypt (around 3200–3000 BC), identified on a protodynastic period bowl with markings attributed to the Scorpion King (MFA #98.1011) [12, 13]. Egyptian blue was a highly desirable blue pigment in Egypt and the Near East used profusely through the late Roman period to create fields of blue on wall paintings, cartonnage, and pottery.

The identification of pigments often requires the removal of microsamples for analytical techniques such as scanning electron microscopy/energy-dispersive X-ray spectroscopy (SEM–EDX), Raman spectroscopy, and XRD. However, the destructive removal of a small sample is not always permissible or possible. Portable XRF is a powerful tool for non-destructive analysis, ensuring the detection of copper associated with Egyptian blue and other copper-based pigments. In the last decade, the development of noninvasive imaging techniques has led to a variety of new tools for the spatial characterization of organic and inorganic materials. Because it can characterize and locate materials on a surface when taking a sample is not an option, near-infrared (NIR) luminescence imaging (also often called visible-induced luminescence, VIL) is particularly suitable for the identification of pigments in museum environment.

In NIR luminescence imaging, the luminescence response of inorganic and organic compounds is recorded in the NIR when excited by visible light [14–16]. This technique is very sensitive to the detection of Egyptian blue, even in amounts too small to be observed with the naked eye [17]. Cuprorivaite exhibits a strong luminescence band at 910 nm when excited by visible light [15–17] due to the symmetrically prohibited $^2B_{1g} \rightarrow {}^2B_{2g}$ electronic transition attributable to the Cu^{2+} ion [15]. Previous work by Verri [16] has exploited this property of Egyptian Blue and has shown the optimal experimental conditions to capture NIR luminescence imaging on museum objects [16, 18–23].

NIR luminescence imaging of the Phoebe Hearst portraits revealed the possible presence of Egyptian blue in areas that were decidedly not blue in appearance: in underdrawings, in modulations of white on clothing, and in gray backgrounds (Fig. 1a, b). This apparent use of a blue pigment in a secondary role on four mummy portraits and one panel from PAHMA warranted investigating whether the observed luminescence resulted exclusively from the presence of Egyptian blue or whether other painting materials and pigments may have contributed to the NIR

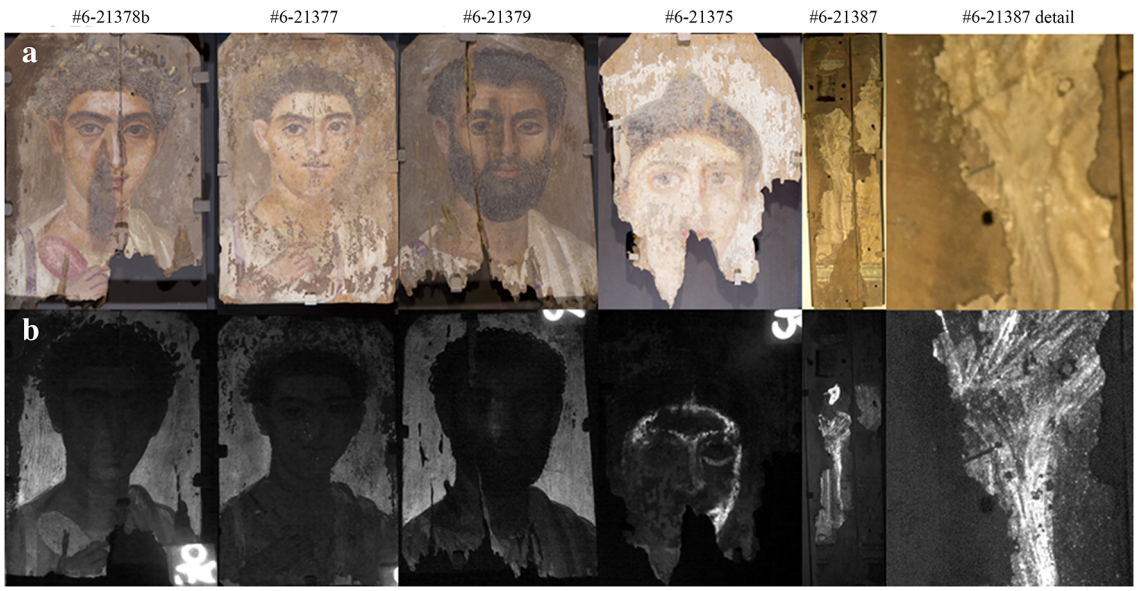

Fig. 1 Portraits from Tebtunis showing a strong luminescence in the near infrared (850–1100 nm). **a** Visible light, **b** near IR

response. As described previously [19], the qualitative nature of NIR imaging means that other supplemental analytical techniques are required to positively identify the Egyptian Blue pigment. Here, we describe the application of a multi-analytical approach using in situ X-ray fluorescence spectrometry (XRF) and X-ray diffraction (XRD), and SEM–EDX on cross section taken from a representative portrait, to identify Egyptian blue on these portraits and better understand the use of this pigment in Roman Egypt.

2 Materials and methods

2.1 Egyptian portraits and paintings

The Egyptian collection of the PAHMA includes a group of fifteen Roman Egyptian portraits and painting fragments. This study focuses on four portraits (portrait of a boy, #6-21377; portrait of a young man, #6-21378b; portrait of a bearded man, #6-21379; portrait of a woman #6-21375) and one painted panel (#6-21387), selected on the basis of their positive luminescence responses in the NIR, as described below (Fig. 1). The three male portraits (#6-21377, #6-21378b, and #6-21379) appear similar in structure and painting style. Each is executed on a 12-mm-thick oak (*Quercus* sp.) panel and has relatively thick and highly textured paint. In the impasto on their faces, tool marks characteristic of heated encaustic application are clearly visible, while on the gray backgrounds surrounding the faces, the paint was applied with a brush. Here, brush strokes and an occasional brush fiber are visible [2]. A small sample was removed from the portrait of a young man, #6-21378b, and embedded in epoxy resin and polished to obtain a cross section. This sample comes from along a loss at the interface between the face, orange pink in color, and the gray background. The female portrait (#6-21375), painted on hackberry (*Celtis* sp.), is less well preserved than the three male portraits, retaining very little of its original surface. Lastly, the painted panel, #6-21387, appears very different from the portraits. The paint is thinly applied over a white ground. The binding medium, which appears to be different from the wax used on the mummy portraits, is currently under investigation.

2.2 NIR luminescence

Luminescence is the emission of light by a substance, which occurs when an electron returns to the electronic ground state from an excited state and loses its excess energy as a photon. In the specific situation when the excitation is caused by photons, then the phenomenon is known as photo-induced luminescence. NIR luminescence focuses on the response of inorganic and organic compounds when excited in the visible range. These include Egyptian blue, which emits a strong luminescence centered at about 910 nm [15–17].

A great advantage of the use of NIR luminescence is the possibility to use off-the-shelf equipment: a visible excitation source, a series of filters, and a recording device with some sensitivity in the 800–1000 nm range. For the experiments here described, radiation source consists of a xenon flashlight. An X-Nite CC1 daylight filter, with a 50 % transmittance efficiency between 325 and 645 nm, was placed in front of the radiation source to eliminate the UV and IR contributions of the light source. A Canon EOS 5D Mark III DSLR camera body modified by removing the IR-blocking filter was used to record the luminescence responses. To select the emission range under investigation, and eliminate the contribution from the visible range, the camera was fitted with an X-Nite850 cut-on filter, with a 50 % transmittance efficiency at ca. 850 nm. To eliminate any possible light contributions other than the filtered flash, the experiment was conducted in a dark room ensured to have no leaks from stray light. A threshold was applied to the histogram of the raw 32-bit image so that random dark noise spikes on the sensor were no longer visible in the non-fluorescing areas of the image (e.g., the matte gray storage container). A ceramic tile painted with laboratory-made Egyptian blue was also included in each image as a secondary check that that our experimental setup was producing a florescence response. While this tile was not used to standardize the fluorescence response, it does indicate the NIR brightness of pure Egyptian blue when exposed to visible light.

2.3 X-ray fluorescence (XRF) spectrometry

X-ray fluorescence spectroscopy provides a fingerprint of the elemental composition of the investigated material. The presence of copper (Cu Kα = 8.047 keV) is diagnostic for Egyptian blue.

XRF analyses were carried out using an ELIO X-ray fluorescence spectrometer (XGLab), equipped with an Rh tube and 1 mm spot size. An integrated CCD camera and two laser pointers allow perfect focus on the desired region of interest. The instruments allows for the collection of both points and maps. All analysis were performed in atmospheric condition. For the current study, point analyses were performed at 40 kV and 100 μA, with a collection time of 120 s. Points have been selected in order to obtain a representation of the different colors distinguishable by the naked eye. Maps were recorded at the intersection of multiple color fields, such as the eye, or in regions defined as significant on the basis of the NIR luminescence imaging, such as the interface between the background and the

tunic. For the maps the instrument was operated at 40 kV and 100 μA. The rastering was executed with a step size of 250 μm and acquisition time of 1 s for each point.

2.4 X-ray diffraction (XRD)

XRD was carried out using a noninvasive, portable XRD/XRF instrument, DUETTO by InXitu/Olympus [24], housed at the Getty Conservation Institute (GCI) in Los Angeles, CA, USA. The instrument is equipped with a Ni-filtered Cu Kα radiation at 10 W power. For the experiments here described, it was operated with a fixed CCD position, a 2θ range of 20°–50°, XRD resolution of 0.3°, and an exposure time of approximately 1 h.

2.5 Optical microscopy

The sample from portrait of a young man #6-21378b, prepared as a cross section, was examined with a polarized light microscope Nikon Eclipse MA200 using a 50× objective. Optical images were captured using an attached Nikon digital sight DS-FI2 camera.

2.6 Scanning electron microscopy (SEM)

Backscattered electron (BSE) images were collected to show the size and distribution of the Egyptian blue pigment particles. Analyses were performed on a carbon-coated cross section taken from a selected portrait considered to be representative for the whole group on the basis of the non-destructive investigations performed systematically on all paintings. The images were acquired using a Hitachi S-3400N-II in high vacuum mode, equipped with an energy-dispersive spectrometer in the NUANCE facility at Northwestern University. The accelerating potential was 20 kV.

3 Results

3.1 NIR luminescence

All 15 Roman Egyptian paintings from the PAHMA collection were investigated by luminescence imaging. However, only four portraits (portrait of a boy, #6-21377; portrait of a young man, #6-21378b; portrait of a bearded man, #6-21379; portrait of a woman #6-21375) and one painted panel (#6-21387) demonstrated strong NIR luminescence. Figure 1a, b, respectively, shows these five paintings in visible light and in the NIR. As a comparison, we have also included a portrait (Fig. 2, #6-21376) that has no observable luminescence in the NIR.

The NIR luminescence on these three male portraits are localized primarily to the background region, where even under high magnification no blue color is discernible. In the portrait of a young man (#6-21378b), a less intense luminescence is also observed in the purple-colored *clavus* (a vertical colored stripe on the tunic) and in the pink 'rose garland' bundle held in the figure's proper right hand. While the luminescence of such areas could indicate the presence of small amounts of Egyptian blue mixed with an organic pink colorant to create the purple shade of these

Fig. 2 Portrait from Tebtunis (#6-21376) with no observable luminescence in the near infrared. The Egyptian blue reference 'CIAO' shows a strong luminescence

areas, it is possible that the observed luminescence is associated with other organic pigments [14, 16, 25].

The female portrait (#6-21375) exhibits a bright luminescence along the contour of the face, as well as the outline of her eyes and nose. The possible use of Egyptian blue here as an under-drawing or shadowing pigment is surprising. Sketches typically would be made with cheaper and more readily available pigments such as carbon black or chalk. Good examples are the chalk drawings observed by Williams [2] on some of the portraits. Even more representative is the incomplete portrait in the Phoebe A. Hearst Museum collection (#6-21378a) where the sketched drawing and writings were made with a carbon-based pigment [2].

In the painted panel, #6-21387, the blue area corresponding to the shaved scalp of the priest figure appears glowing white in the NIR luminescence image. The luminescence is also observed throughout the priest's white mantle and tunic where the paint color could have been modulated with Egyptian blue to give this cloth shadow and form or, instead, served as an under-drawing.

To confirm the presence of Egyptian blue in each of the above areas where NIR luminescence was observed, complementary analysis was performed with X-ray fluorescence (XRF) and X-ray diffraction (XRD).

3.2 XRF mapping and point analyses

Guided by the NIR luminescence results, XRF maps were collected on the three male portraits (#6-21377, #6-21378b, and #6-21379) in a rectangular area where the gray background, the white tunic, and its purple *clavus* intersect. The response of #6-21378b to both NIR luminescence and XRF in this region is representative of all three portraits. Figure 3a indicates the location of the XRF map (demarcated by a rectangle) on #6-21378b. Figure 3b, c, respectively, shows the visible and NIR images of this local area. Figure 3d–g shows the XRF intensity distributions of the Kα X-ray bands for Cu, Fe, Ca and the Lα band of Pb. Shown as heat maps, the blue in these figures indicates low amounts or the absence of a particular element, red indicates high concentrations, and intermediate concentrations are shown in green and yellow. Comparisons of relative concentrations between each of these elemental distribution images are not possible since no steps were taken to normalize or quantify the peak intensities.

In Fig. 3c, the gray background luminesces brightly in the NIR that is colocated with a Cu-rich region of the X-ray map (Fig. 3d) providing evidence that the luminescence is caused by a Cu pigment, very likely Egyptian blue. However, a moderate NIR luminescence response is also observed in the purple *clavus*, but this region has weak Cu intensities in the XRF map suggesting only background levels of this metal. Finally, the white tunic does not luminesce at all nor does it contain detectable Cu all of which indicates an absence of Egyptian blue. Since appreciable Cu was not be detected in the *clavus* nor tunic, this suggests that the luminescence properties of this purple stripe are instead be associated with other organic or inorganic compounds rather than Egyptian blue to create this color.

NIR luminescence images of the female portrait (#6-21375) and painted panel (#6-21387) in Fig. 4a, b indicate other areas of fluorescence which warranted deeper

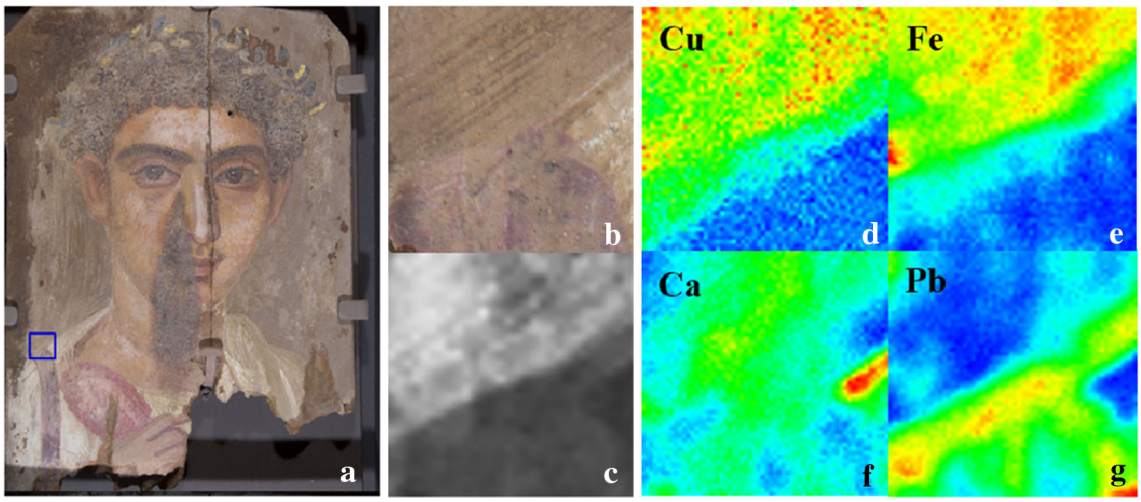

Fig. 3 Portrait of a man (#6-21378b). From the *left*: **a** visible light image of the painting. In the *squares*, close up images of the mapped area. **b** Visible light and **c** NIR luminescence image. A strong response is observed in correspondence with the *gray* background, while a weak luminescence is shown by the *purple clavus*. On the *right*, **d**–**g** XRF intensity distributions of the Kα X-ray bands for Cu, Fe, Ca and the Lα band of Pb. High concentration of Cu is observed in correspondence with the *gray* background

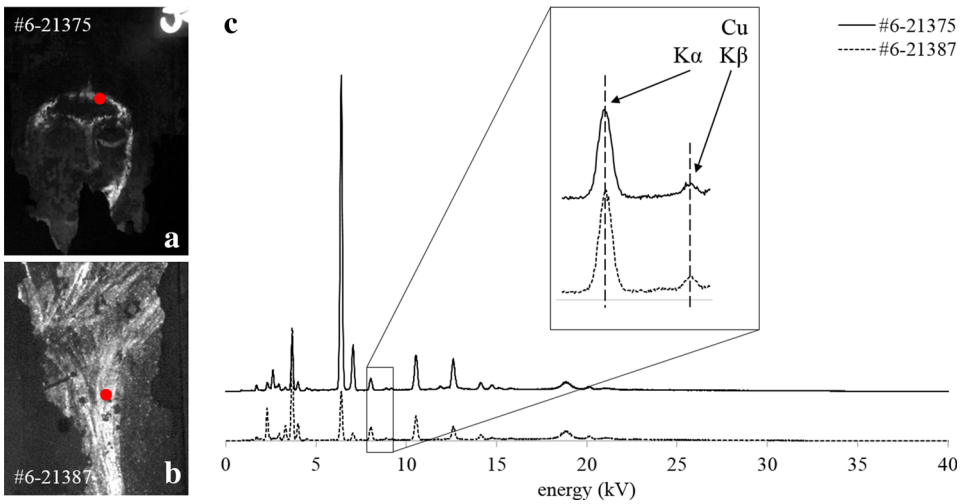

Fig. 4 XRF point analysis. On the *left*, NIR luminescence images for paintings **a** #6-21375 and **b** #6-21387. On the *right*, point analysis taken on the spots shown in *red*. The *close up area* shows the Kα and Kβ peaks of Cu at 8.047 and 8.905 eV

investigation by XRF. In Fig. 4c, representative XRF spectra from the forehead along the hairline of the female portrait and a purplish point on the mantle for the painting fragment both show Cu Kα and Kβ peaks supporting the presence of Egyptian blue in these areas.

3.3 In situ XRD

XRD is an excellent tool for the identification of Egyptian blue since it can identify the crystalline-phase cuprorivaite, which provides Egyptian blue with its color [26]. XRD analyses were performed on the three male portraits (#6-21377, #6-21378b, and #6-21379) and on the painted panel (#6-21387), in areas where the presence of Egyptian blue was suggested by NIR luminescence imaging. On some objects in this study (such as #6-21375), the block-like geometry of the diffractometer and the curvature of the object made analysis with this instrument impossible.

As may be observed in Fig. 5, the general patterns obtained from all of these analyses are similar, pointing to the use of common materials in the different paintings. However, the identification and assignment of the peaks to specific crystalline phases are less straightforward. The heterogeneity and uneven texture of the paint affect the in situ XRD analyses, causing a shift in the diffraction patterns relative to the library standards. The curvature of panels further complicates the peak identifications, introducing a non-constant shift throughout the 2θ regions. Figure 5 shows diffraction patterns from the portrait of a young man (#6-21378b) and the painted panel (#6-21387). Figure 5a, b reports the diffraction patterns for #6-21378b, collected on the cheek (Fig. 5a) and on the gray background (Fig. 5b). On the cheek, where no NIR luminescence was observed, no cuprorivaite is detected. Conversely, XRD pattern for the gray background (Fig. 5b) shows the presence, although weak in intensity, of cuprorivaite peaks, together with jarosite [$KFe^{3+3}(SO_4)_2(OH)_6$]. Similarly, diffraction patterns collected on the painted panel (#6-21387) are shown in Fig. 5c, d. In this case, the diffraction pattern obtained on the blue scalp (Fig. 5d) shows a more intense cuprorivaite peak, together with jarosite and cerussite ($PbCO_3$), as noted by the appropriate peaks. By comparison, the XRD pattern (shown in Fig. 5c) from an area of red paint on the panel that did not luminesce in the NIR does not include the characteristic peaks for cuprorivaite.

3.4 Polarized light microscopy and SEM–EDX analyses of a paint cross section

A small sample was removed from the portrait of a young man, #6-21378b, along a loss at the interface between the face, orange pink in color, and the gray background (Fig. 6). Microscopic observation of the polished cross section (Fig. 6a) shows a complex mixture, with two main, not clearly defined layers: a whitish beige layer and a slightly more intense light brown. Both parts contain inclusions that vary widely in color (white, white-off, red, bright yellow, and black), shape (from rather rounded to the more angular black inclusions), and size (ranging from <1 μ to a maximum of 13 μm) (Fig. 6b). SEM–EDX analyses of the white inclusions find a concentration of lead, while the white-off inclusions show high amounts of iron and sulfur. Red and bright yellow inclusions are iron based. A single large brown inclusion of about 18 μm containing calcium and sulfur is also present. Certain inclusions appear translucent, with characteristic elongated shapes (Fig. 6c) up to 10–13 μm in length. The morphology and elemental composition of these particles, with high amounts of silicon, together with calcium and copper (Fig. 6d), are typical of cuprorivaite crystals, pointing to the presence of Egyptian blue.

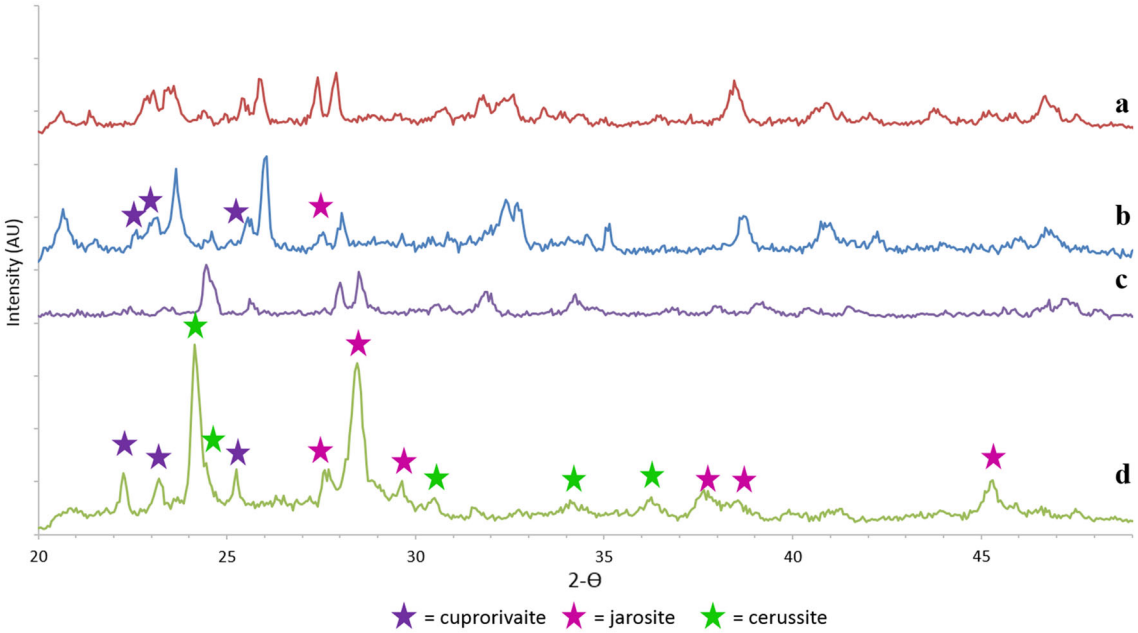

Fig. 5 XRD patterns for the portrait of a young man (#6-21378b) and the painting fragment (#6-21387). **a** Cheek of #6-21378b, no cuprorivaite; **b** *gray* background of #6-21378b, small peak of cuprorivaite together with jarusite; **c** *red* area of #6-21387, no cuprorivaite; **d** *blue* hair of #6-21387, with cuprorivaite, jarusite, and cerussite

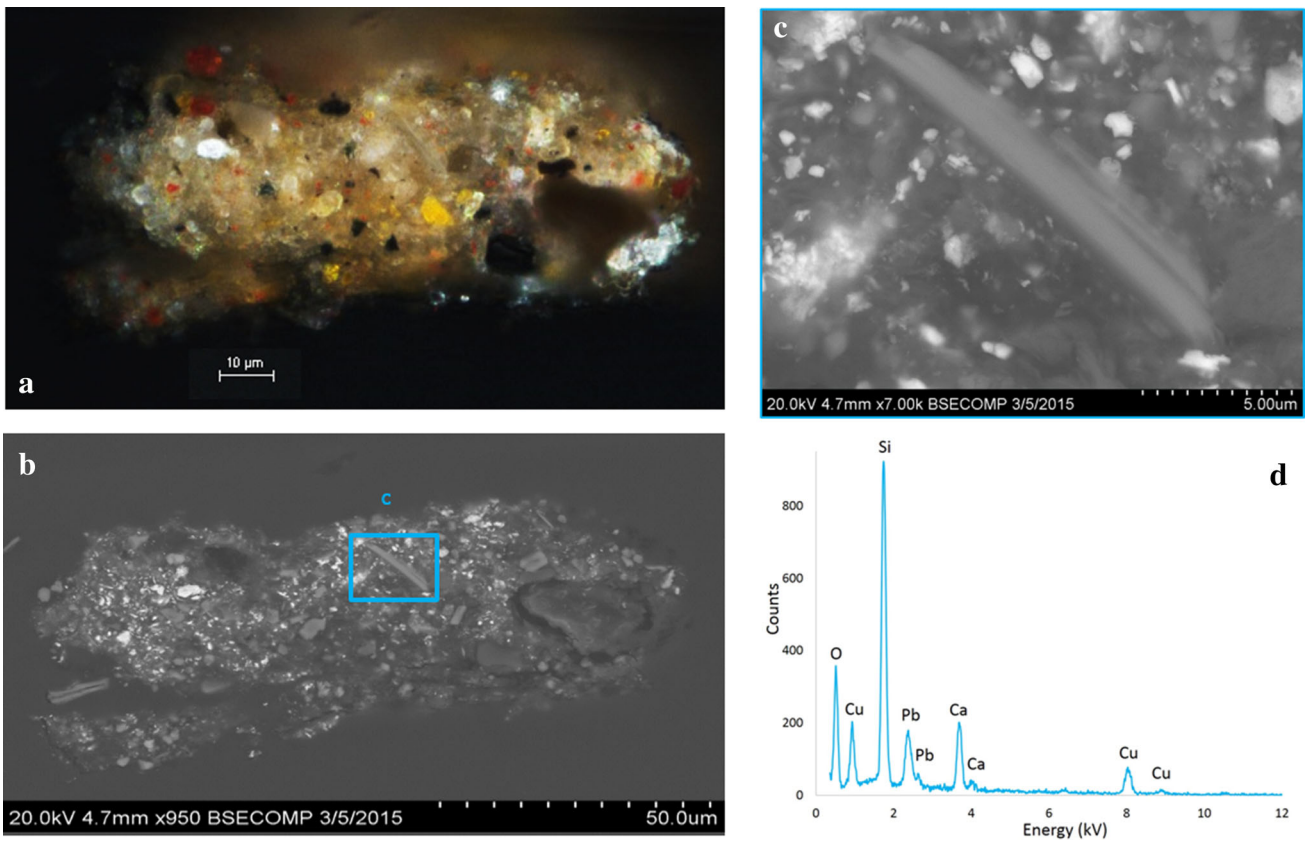

Fig. 6 Fragment from the portrait of a young man (#6-21378b) polished as cross section: **a** optical image of cross section, showing a complex layer; **b** backscatter SEM image, exhibiting the presence of copper-rich large elongated inclusion; **c** high-magnification backscatter SEM image of copper-rich elongated inclusions; **d** corresponding EDX spectra

4 Discussion

It is important to emphasize that Egyptian blue has a luminescence peak centered at 910 nm [15, 17]. However, NIR luminescence is not wavelength specific and thus cannot be used as an analytical technique by itself to identify Egyptian blue. Excitation for NIR imaging occurs over a broad range, from 300 to 700 nm, and the luminescence phenomenon is recorded in the NIR region, 850 to 1100 nm. As will be discussed in more depth below, a weak response could also be recorded in the lower detection range as tails from bands that show visible luminescence just below the cutoff wavelength [25], questioning the specificity of NIR luminescence imaging to just Egyptian blue.

As shown in Fig. 1, only five (#6-21375, #6-21377, #6-21378b, #6-21379, and #6-21387) of the Tebtunis Roman Egyptian paintings investigated here have an observable NIR luminescence response, suggesting the presence of Egyptian blue. The variation in luminescence intensity needs special attention. Pure Egyptian blue is characterized by a very bright, glowing white emission in the NIR, as shown by the Egyptian blue reference tile (CIAO) present in all recorded images (Figs. 1b, 2). The modulation in the luminescence intensities observed on these paintings is probably associated with the use of Egyptian blue not as pure pigment but as part of a mixture. Although it is plausible that Egyptian blue was mixed with an organic dye to mimic expensive colorants used in textiles, the possibility of a luminescence response from the dye itself cannot be excluded. A test study from Verri [22] indeed suggests that other inorganic and organic pigments might show a luminescence response in the near IR when excited in the visible range. Cadmium-based pigments, later in date and of little interest for the present study, can luminesce as strongly as Egyptian blue [22]. In addition, certain lake pigments, such as madder and kermes, mixed with lead white might show a weak to moderate NIR luminescence response [22]. In addition, indigo has an emission peak centered at 750 nm [14, 16], while purpurin and pseudopurpurin show a peak tail in the 800 nm region [25]. The purple *clavus* is an example. Although this area is characterized by a weak luminescence, as shown in Figs. 1b and 3c, the absence of detectable amount of Cu in the map obtained by XRF (Fig. 3d) may exclude the use of Egyptian blue, leaving an open question regarding the nature and attributions of such luminescence which is the subject of ongoing investigation.

Results obtained on the Tebtunis Roman Egyptian paintings also offer some new insights into the ancient painting techniques. Egyptian blue is a toning agent added to gray background (#6-21377, #6-21378b, and #6-21379), modulates the color of a white tunic and mantle (#6-21387), and appears in an under-drawing outlining a face (#6-21375). In situ XRF and XRD confirm the identification of Egyptian blue on these paintings. XRF mapping clearly indicates the presence of Cu in the gray background (Fig. 3a) and its absence on the tunic. XRD further confirms this identification, as it specifically detects cuprorivaite in the gray background (Fig. 5b). Lastly, Egyptian blue particles can be identified by their characteristic morphology (translucent, elongated crystals) and elemental composition (high in Si, Ca, and Cu) in a polished cross section from the gray background of #6-21378b. The particles are few, but dispersed throughout the rich mixture of pigments comprising the gray paint layer (Fig. 6).

These unusual occurrences of Egyptian blue in these Roman Egyptian paintings with no outwardly visible blue color could be attributed to the glassy matrix of the Egyptian blue or to other qualities that were appreciated and specifically selected, perhaps to impart brightness to the gray background of the male portraits (#6-21377, #6-21378b, #6-21379). The use of Egyptian blue as under-drawing pigment (as in the female portrait #6-21375) introduces questions about the wide availability of Egyptian blue during the Roman period, suggesting it was so abundant that it could be a substitute for carbon black or chalk.

Finally, the uses of Egyptian blue described in this study could also indicate that the pigment was no longer a prized material in the palette of the Roman Egyptian painters. There is some evidence for a Greco-Roman disregard for blue as described by Pliny the Elder, in the *Naturalis Historiae* (book XXXV, 32). Greek tetrachromy involves the use of a very limited palette, made of only four colors: white from Melos, Attic yellow, red from Sinope on the Black Sea, and the black called *atramentum* [27]. Surprisingly, blue is not mentioned in this list.

Blue was of course known and available, but it was used only where appropriate [28]. Bruno [29] for instance suggests that Greek artists would consider blue not as a color but as a darkener, used to modify the aspect of the other pigments. Pliny the Elder (book XXXII, 57) mentions the use of more than one blue material (ceruleum) from Egypt, Iran (Schythians), and Cyprus, used to create shadows (book XXXV, 11). The similar use of Egyptian blue observed in the Tebtunis paintings (i.e., in the gray paint of the background or in the shading of the tunic) suggests a strong connection to these Greek painting traditions.

5 Conclusions

The fifteen Tebtunis Roman Egyptian portraits in the collection of the Phoebe A. Hearst Museum of Anthropology (PAHMA) at the University of California, Berkeley, have

been investigated with the aim of identifying and spatially locating the pigment Egyptian blue.

NIR luminescence imaging has proven to be a powerful, noninvasive tool for the identification of this blue pigment. Complementary analyses by in situ XRF and XRD, and SEM–EDX analysis of a cross section confirmed the presence of Egyptian blue in each of the areas where a bright luminescence was recorded. However, the purple stripes and pink garland of the three male portraits exhibited a fainter luminescence in near IR, and complementary analyses did not confirm Egyptian blue in these areas. Further studies are needed to better understand the luminescence properties of other inorganic and organic pigments.

The unexpected uses of Egyptian blue observed here, as toning agent added to the gray background or to modulate the white of clothing, and as an under-drawing pigment used to outline the face, offer new insights into ancient painting techniques during the Roman period.

Acknowledgments Research at the Northwestern University/Art Institute of Chicago Center for Scientific Studies in the Arts (NU-ACCESS) is supported by generous grant from the Andrew W. Mellon Foundation. This work made use of the EPIC facility (NUANCE Center-Northwestern University), which has received support from the MRSEC program (NSF DMR-1121262) at the Materials Research Center; the Nanoscale Science and Engineering Center (NSF EEC-0647560) at the International Institute for Nanotechnology; and the State of Illinois, through the International Institute for Nanotechnology.

References

1. N. Thomson, *American Discovery of Ancient Egypt* (Los Angeles County Museum of Art, Los Angeles, 1995), pp. 56–58
2. J. Williams, in *Decorated Surfaces on Ancient Egyptian Objects: Technology, Deterioration and Conservation*, ed. by J. Dawson, C. Rozeik, M. Wright (Archetype, London, 2010), pp. 127–138
3. N. Marlowe, *Catalog of the Painted Portraits from Roman Egypt in the Lowie Museum Collection* (University of California, Berkeley, 1982)
4. A. Walker, *Notes on Mummy Portraits and Other Finds from Grenfell and Hunt's Excavation at Tebtunis (1899–1900), Now in the Phoebe Hearst Museum of Anthropology* (University of California, Berkeley, 1998)
5. S. Walker, M. Bierbrier, *Ancient Faces: Mummy portraits from Roman Egypt* (Trustees of the British Museum, London, 1997)
6. A. Pabst, Acta Crystallogr. **12**, 733–739 (1959)
7. F. Mazzi, A. Pabst, Am. Mineral. **47**, 409–411 (1962)
8. H. Jaksch, W. Seipel, K.L. Weiner, K.L. Weiner, A. El Goresy, Die Naturwissenschaften **70**, 525–535 (1983)
9. T. Pradell, N. Salvado, G.D. Hatton, M.S. Tite, J. Am. Ceram. Soc. **83**, 1426–1431 (2006)
10. M.S. Tite, M. Bimson, N.D. Meeks, Rev. Archeom. **1**, 297–301 (1981)
11. P. Bianchetti, F. Talarico, M.G. Vigliano, M.F. Aali, J. Cult. Herit. **1**, 679–692 (2000)
12. M.K. Hartwig, *A Companion to Ancient Egyptian Art* (Wiley, London, 2014)
13. J.E. Quibell, F.W. Green, W.M.F. Petrie, *Hierakonpolis: Plates of Discoveries in 1898* (Egyptian Research Account, London, 1900)
14. D. Ajo', G. Chiari, F. De Zuane, M. Favaro, M. Bertolin, in *Art '96 Proceedings of the 5th International Conference on Non-Destructive Testing, Microanalytical Methods and Environmental Evaluation for Study and Conservation of Works of Art* (Budapest, 1996)
15. G. Pozza, D. Ajo', G. Chiari, F. De Zuane, M. Favaro, J. Cult. Herit. **1**, 393–398 (2000)
16. G. Verri, Anal. Bioanal. Chem. **394**, 1011–1021 (2009)
17. G. Accorsi, G. Verri, M. Bolognesi, N. Armaroli, C. Clementi, C. Miliani, A. Romani, Chem. Commun. 3392–3394 (2009). doi:10.1039/b902563d
18. G. Verri, in *Proceedings of the SPIE*, vol. 7391, ed. by L. Pezzati, R. Salimbeni. O3A, Optics for Arts, Architecture, and Archaeology II (2009), p. 739105
19. G. Verri, P. Collins, J. Ambers, T. Sweek, S.J. Simpson, Br. Mus. Tech. Res. Bull. **3**, 57–62 (2009)
20. G. Verri, M. Gleba, J. Swaddling, T. Long, J. Ambers, T. Munden, Br. Mus. Tech. Res. Bull. **8**, 59–71 (2014)
21. G. Verri, T. Opper, L. Lazzarini, in *Diversamente bianco. La policromia della scultura romana*, ed. by P. Liverani, U. Santamaria (Edizioni Quasar, Rome, 2014)
22. G. Verri, D. Saunders, Br. Mus. Tech. Res. Bull. **8**, 83–92 (2014)
23. M. Smirniou, G. Verri, P. Roberts, A. Meek, M. Spataro, Br. Mus. Tech. Res. Bull. **4**, 67–78 (2010)
24. P. Sarrazin, G. Chiari, M. Gailhanou, Adv. X-ray Anal. **52**, 175–186 (2008)
25. A. Claro, M.J. Melo, S. Schafer, S. Seixtas de Melo, F. Pina, K.J. Van den Berg, A. Burnstock, Talanta **74**, 922–929 (2009)
26. C. Minguzzi, Period. Mineral. **9**, 333 (1938)
27. R.L.J. Lee, A.B. Fraser, *The Rainbow Bridge: Rainbows in Art, Myth, and Science* (Pennsylvania State University Press, University Park, 2001)
28. J.L. Benson, *Greek Color Theory and the Four Elements. A Cosmological Interpretation* (University of Massachusetts Amherst Libraries, Amherst, 2000)
29. V.J. Bruno, *Form and Color in Greek Paintings* (W. W. Norton, New York, 1977)